INGENIERIA Y COMPETITIVIDAD
REVISTA CIENTÍFICA Y TECNOLÓGICA

Vol.21 No.2 - ISSN: 0123-3033 - DOI: 10.25100/iyc.v21i2.8105

CHEMICAL ENGINEERING

Modeling of a Solar Heterogeneous Photocatalytic Reactor with TiO_2 for Treatment of Wastewater Contaminated By Albendazole

INGENIERIA QUIMICA

Modelado de un Reactor Solar Fotocatalítico Heterogéneo con TiO_2 para el Tratamiento de Agua Residual Contaminada con Albendazol

María Margarita-Guerra[1], Rodinson Arrieta-Pérez[2], José Colina-Marquez[1§]

[1] Universidad de Cartagena, Departamento de Ingeniería Química, Cartagena, Colombia

[2] Universidad de Puerto Rico, Departamento de Ingeniería Química,

San Juan de Puerto Rico, Puerto Rico

mmargaritaguerra@hotmail.com, rodinsonarrieta@hotmail.com, [§]jcolinam@unicartagena.edu.co

(Recibido: 04 de Junio de 2019 – Aceptado: 30 de Junio de 2019)

Abstract

Albendazole is an anthelmintic drug with antiangiogenic properties, which means that inhibits the development of new blood vessels. This causes a serious risk for the growth of fetus during pregnancy as a result. Heterogeneous photocatalysis has been proposed as an alternative for removal of this contaminant. In this study, a solar compound parabolic collector (CPC) photocatalytic reactor was modeled and simulated in order to describe the total organic carbon (TOC) degradation of commercial albendazole. The Six Flux Model approach (SFM) was used to estimate the Local Velocity Volumetric Rate of Photon Absorption (LVRPA) coupled with a Langmuir-Hinshelwood (L-H) kinetic model in order to describe the photocatalytic degradation of the TOC content of the contaminant and its photochemical oxidation products. The parameters of the L-H model were estimated from experimental data obtained with a catalyst loading of 0.6 g/l, initial pH of 5.0 and three different initial TOC concentrations of the commercial albendazole (159.95, 75.58 and 40 ppm). The rate constant (k_T) and adsorption constant (K_1), estimated from the parameter fitting, were 9.28×10^{-4} $m^{1.5}ppmW^{-0.5}$ s^{-1} and 3.02×10^{-2} ppm^{-1}, respectively. The model was validated with experimental results, achieving a TOC removal of 40% with the lowest concentration of the contaminant. By simulating the process with different catalyst loadings, the maximum TOC removal was achieved with 0.21 g/L of TiO_2.

Keywords: Langmuir-Hinshelwood, CPC, LVRPA, Emergent pollutants, SFM.

Resumen

El albendazol es un medicamento anthelmíntico con propiedades antiangiogénicas, lo que significa que inhibe el desarrollo de nuevos vasos sanguíneos. Esto implica un riesgo serio para el crecimiento del feto durante el embarazo. La fotocatálisis heterogénea se ha propuesto como alternativa para eliminar este contaminante emergente. En este estudio, un reactor fotocatalítico solar de collector parabólico compuesto (CPC) se modeló y simuló para describir la degradación del carbono orgánico total (TOC) del albendazol comercial. El enfoque del modelo de seis flujos (SFM) se empleó para calcular la velocidad local volumétrica de absorción de fotones (LVRPA) y se acopló con el modelo cinético de Langmuir-Hinshelwood (L-H) para describir la degradación fotocatalítica del contenido de TOC de el contaminante y los productos de su oxidación. Los parámetros del modelo L-H se estimaron a partir de datos experimentales obtenidos con una carga de catalizador de 0.6 g/l, un pH inicial de 5.0 y tres diferentes concentraciones iniciales de TOC del albendazol comercial (159.95, 75.58 y 40 ppm). La constante cinética (k_T) y la constant de adsorción (K_1), calculadas a partir del ajuste de parámetros fueron 9.28×10^{-4} $m^{1.5}ppmW^{-0.5}$ s^{-1} y 3.02×10^{-2} ppm^{-1}, respectivamente. El modelo se validó con resultados experimentales, alcanzando una reducción de TOC del 40% con la concentración más baja del contaminante. Simulando el proceso con diferentes cargas de catalizador, la máxima reducción de TOC se obtuvo con 0.21 g/L de TiO_2.

Palabras Clave: Langmuir-Hinshelwood, CPC, LVRPA, Contaminantes emergentes, SFM

1. Introduction

Solar heterogeneous photocatalysis, based on TiO_2, has showed to be an effective treatment for the removal of many emerging contaminants from industrial wastewater [1,2]. Pharmaceutical residues are considered as emerging pollutants and they are resistant to conventional biological treatments, so the solar heterogeneous photocatalysis has been used as an alternative to remove these compounds and their metabolites [3, 4].

Pharmaceutical contamination has become a relevant topic, due to the damage that these compounds may cause to aquatic ecosystems. In some cases, it was observed that there was feminization of some fish species that have been exposed to estrogen concentrations lower than 10 ppm [5]. Also, the appearance of drug-resistant bacterial strains, specifically to antibiotics, has been associated with residues that have appeared in water surfaces [6]. Anthelmintic drug residues, have been found in chicken eggs [7], and may have antiangiogenic favorable for cancer treatment, but harmful to gestation stage because they inhibit the growth of blood vessels in fetus [8]. Although, there are no public reports about health problems related to contamination of water surface bodies with pharmaceutical residues, some isolated cases whose origin may be the exposure or ingestion of pharmaceutical residues from drinking water has been reported [9].

Several studies have reported promising results about the performance of solar heterogeneous photocatalysis as an alternative treatment of these contaminants. Some drugs, such as naproxen or antihistamines, have been submitted to photocatalytic degradation using polycrystalline TiO_2, with very acceptable results. Furthermore, the photocatalytic degradation of ibuprofen has been analyzed in previous studies [10, 11]. However, all these studies were carried out at lab scale and the applicability of solar heterogeneous photocatalysis of pharmaceutical compounds at larger scales depends on appropriate process modeling and simulation in order to determine the physical requirements of a full-scale facility.

One of the main challenges of photocatalysis, from a commercially applicable perspective, is the lack of kinetic models that allow scaling up photocatalytic reactors properly. The difficulty in studying this kind of systems is that the photonic component must be coupled with the

reaction kinetics law. Some mathematical approaches have been proposed to solve this problem. The rigorous approach, with the numerical solution of the radiative transfer equation (RTE), was proposed as a very good approximation to the behavior of photoreactors [12]. However, this approach requires considerable computing time and it has been validated under highly controlled experimental conditions. This becomes a very limiting aspect regarding to the model applicability in several types of photocatalytic reactors, especially those that use solar radiation for promoting redox reactions [13, 1].

Li Puma *et al.* [14] proposed a simplified approach for calculating the photonic component by the SFM and coupling it to a L-H kinetic law. The semi-empirical model fitted satisfactorily to experimental data from lab scale photoreactors with artificial UV radiation. Colina-Marquez *et al.* [15] adapted this approach for fitting to experimental data obtained with pilot-scale CPC solar reactors used for degrading a mixture of commercial pesticides. A more recent study developed by Mueses *et al.* [16] proposed a model that introduced the concept of the effective radiant field, which was successfully validated with experimental data reported in previous works, such as: dichloracetic acid, 17-β estradiol and 4-chlorophenol.

This study used the approach adapted by Colina-Marquez *et al.* [15, 17] for describing the kinetics of the photocatalytic degradation of commercial albendazole in a pilot scale solar CPC reactor. The results obtained in this study showed a good fitting to the experimental data, regarding to TOC removal of the commercial drug and its oxidation byproducts degradation. In addition, an optimal catalyst load (0.21 g/L) was obtained from simulating the solar photoreactor.

2. Materials and Methods

2.1. Materials

The pilot-scale CPC photoreactor used in this study is shown in Figure 1. It consisted of 10 glass tubes SCHOTT Duran ® of 32 mm of outside diameter, 1.4 mm of wall thickness and 1.27 m of length, organized in five rows onto compound parabolic collectors, made of aluminum of high reflectivity (85%) [18]. This assembly was supported by a metal structure. The CPC reactor was located at the Laboratory for Solar Photocatalysis of the Universidad del Valle.

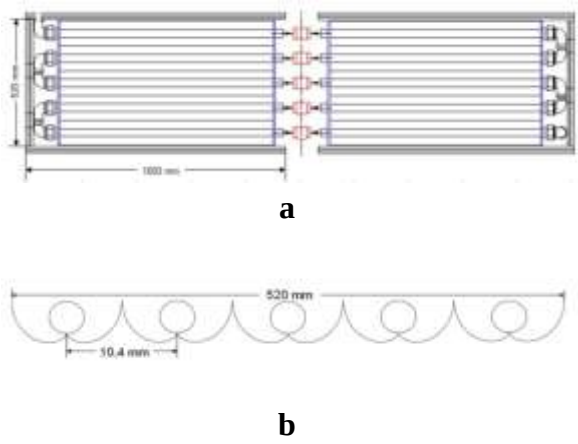

a

b

Figure 1. *CPC photoreactor: principal structure. (a) General Scheme, (b) Cross-section view*[19]

A 0.5 HP nominal power centrifugal pump delivered the recycling flow, from the feed tank and through the system, releasing a maximum flow-rate of 35 $L \cdot min^{-1}$ and assuring the turbulent regime. The flow-rate was kept at an average value of 30 $L \cdot min^{-1}$.

The solutions for pilot-scale tests were prepared with 20L of tap water and commercial preparation of albendazole (La Santé 400 mg/20ml). The TOC initial concentrations used for this study were set at the following values: 159, 95, 75, 58 and 40 ppm, which correspond to the concentration range found in the wastewater of the Laboratory of Pharmaceutical Sciences in the Universidad de Cartagena.

The catalyst used in this study was the commercial TiO_2 Evonik® P-25 (particle size, 20-30 nm by TEM, surface area of 52 m^2/g by BET and a composition of 78% anatase and 22% rutile by XRD). The catalyst loading used was 0.6 g/l and the initial pH was set at 5.0 by using HCl 0.1 N and NaOH 0.1 N solutions. Experimental tests were carried out in late September 2011, with sunny weather conditions. The intensity and the accumulated UV solar radiation (within the 295-380 nm interval) was measured with the radiometer UV Acadus S50.

The slurry with the catalyst was recirculated for five minutes before being exposed to solar radiation in order to guarantee the adsorption-desorption equilibrium. Then, the system was irradiated until the solar UV accumulated energy reached 35 $W \cdot h/m^2$. Samples were taken every 5 $W \cdot h/m^2$ and then, they were centrifuged. The clear liquid of the samples was analyzed with a Shimadzu TOC-VCPH analyzer for measuring the TOC content.

2.2. Photoreactor modeling for albendazole treatment

The mathematical approach used in this work includes combination of several sub-models such as: emission/incidence, absorption (SFM), kinetic and dynamic fluid models, as suggested by Colina-Marquez *et al.* [20].

2.2.1. Six Flux Model

Six Flux Absorption Scattering Model allows analytical estimation of LVRPA in each point of the reactor, considering the photon is absorbed or scattered when it collides with a catalyst particle, following the route of one of the six directions of the Cartesian plane [21]. This model contemplates uniform distribution of catalyst particles in suspension and invariant optical characteristics; negligible absorption of energy by fluid or reactor walls; solar UV radiation absorbed by the photocatalyst (TiO_2) of wavelength between 295 and 384 nm (anatase band gap); constant reflectivity of the reflector surface [17, 22].

Due to the average intensity of UV solar radiation varies with time of year, geographical location and atmospheric conditions. Photocatalytic treatment time was standardized based on a constant solar radiation intensity of 30 W/m^2 [15], which corresponds to the average intensity achieved on a sunny day.

The most important optical parameter considered in the SFM is scattering albedo (ω) of the TiO_2 suspension. This parameter depends on the wavelength of the energy spectrum and it has been reported for several types of TiO_2 catalysts, including P-25 used in this study.

Equation 1 is the LVRPA estimated from the SFM in direction of the incident photon flux.

$$LVRPA = \frac{I_0}{\lambda_{\omega corr}\omega_{corr}(1-\gamma)}\left[(\omega_{corr}-1+\sqrt{1-\omega_{corr}^2})e^{-\frac{r_p}{\lambda_{\omega corr}}}+\gamma(\omega_{corr}-1-\sqrt{1-\omega_{corr}^2})e^{\frac{r_p}{\lambda_{\omega corr}}}\right] \quad (1)$$

I_0 in the equation corresponds to the component of solar radiation reaching the reactor walls, (direct or diffuse radiation). ω_{corr} is the corrected scattering albedo, $\lambda_{\omega corr}$ is the extinction length and r_p is the distance of traveling of the incident photon flux.

Finally, $LVRPA_{r,\theta}$, at a specific location (r, θ) in the reaction space was the sum of the *LVRPA* estimated from each radiation component (direct and diffuse and reflected radiation by these two components) [15].

2.2.2. Reaction Kinetics

In most cases, the kinetic study concludes that degradation rate on the reaction depends on the concentration of pollutant adsorbed according to the Langmuir-Hinshelwood kinetics [21].

For heterogeneous photocatalytic system, the kinetic model based on the reaction mechanism and the absorption rate of radiant energy, is expressed as follows in the Equation 2:

$$-r_{TOC} = k_T(LVRPA)^m \frac{K[TOC]}{1+K[TOC]_0} \quad (2)$$

Where k_T, is the kinetic constant, and K is the binding constant associated to the adsorption of the drug onto the catalyst surface; m takes a value between 0.5 y 1 and depends on the efficiency of electron-hole formation and recombination at the catalyst's surface [20].

2.2.3. Model fluid dynamics

Pilot-scale CPC photoreactors have operated TiO_2 suspensions in turbulent flow regime (Re> 10000) [20, 23]. This avoids mass transfer limitations and catalyst sedimentation.

Some of the assumptions for the approach of the fluid dynamics within photocatalytic reactors are given below:

Liquid is considered as a Newtonian fluid with constant physical properties; steady state operation; catalyst particles are uniformly distributed in the liquid, constant physical and rheological properties of the suspension; the entrainment of bubbles is limited and the effect of velocity gradients in the particles radial distribution are not considered [21].

Literature describes the velocity profile of the fluid as indicated in the Equation 3 and Equation 4:

$$v_z^* = \frac{v_z}{v_z^{max}} \quad (3)$$

Where,

$$\frac{v_z}{v_z^{max}} = \left(1 - \frac{r}{R}\right)^{1/n} \quad (4)$$

R is the reactor radius, v_z^{max} is the maximum fluid velocity into the reactor and n is a parameter which can be calculated as follows (Equation 5):

$$n = 0.41\sqrt{\frac{8}{f}} \quad (5)$$

Where f is the friction factor.

3. Discussion of results

3.1. Solar Radiation Parameters

Solar radiation parameters were taken from previous studies carried out under the same irradiation conditions and in the same reactor geometry.

3.2. Estimating LVRPA

Optical parameters were calculated from the optical properties of the catalyst, as well as the solar radiation spectrum within the reactor, and results are summarized on Table 1. These parameters allowed the determination of the reaction time at each point in photocatalytic reactor space, using a code in the Visual Basic program developed by Colina-Márquez [15] and modified it in this work to fit to the experimental conditions.

Table 1. *Optical Parameters*

Parameters	Unit	Value
Specific mass absorption coefficient, κ	m^2/kg	174.74
Specific mass scattering coefficient, σ	m^2/kg	1295.7
Scattering albedo, ω	dimensionless	0.88
SFM parameter, a	dimensionless	0.87
SFM parameter, b	dimensionless	0.66
Scattering corrected albedo, ω_{corr}	dimensionless	0.75
Extinction length, λ_{wcorr}	m	1.98×10^{-3}

Results obtained, showed the importance of solar collectors, which concentrate solar radiation

within the reactor, permitting a better photonic distribution and consequently, improving photonic availability in the reactor. Similar works have analyzed the presence of the collectors in the CPC solar reactors. Although it is evident that the presence of the reflective screen improves the usage of the UV photons [24-26], there is an interesting approach where the use of other distribution of the tubes (without collectors) can achieve better results than the CPC reactors with the same footprint [27]. Inherently, more conclusive results are needed for getting a clearer idea about the need of solar collectors for photocatalytic applications.

3.3. Kinetic parameters

The initial velocity method, allowed finding kinetic parameters. The equation resulting from the combination of reaction rate law and the material balance in the reactor is Equation 6, written as follows:

$$\frac{1}{V_T\left(-\frac{dTOC}{dt_{30\,w}}\right)_{t=0}} = \frac{1}{k_T K_1 \int_{V_r}(LVRPA)^m dV_r}\left(\frac{1}{TOC_0}\right) + \frac{1}{k_T \int_{V_r}(LVRPA)^m dV_r} \quad (6)$$

From a plot of the inverse initial rate versus the inverse pollutant concentration, the kinetic parameter obtained were K_1 and k_T, as the intercept and slope, respectively. The values obtained are summarized in Table 2.

Table 2. Experimental parameters of L-H equation

	m	**b**	K_1	k_t	$K_1/120\,00$	$k_t/120\,00$
Unit	s/m^3	$s/ppm\ m^3$	1/ppm	$ppm\ m^{1,5}/s\ W^{0,5}$	L/mol	$mol\ m^{1,5}/L\ s\ W^{0,5}$
Value	34,766	1050.4	3.02×10^{-2}	9.28×10^{-4}	368.22	7.74×10^{-8}

Figure 2 shows the graph of the inverse initial concentration and inverse initial rate, according to experimental conditions described above. Linear regression revealed a correlation factor of 0.973, showing a good fitting of the data.

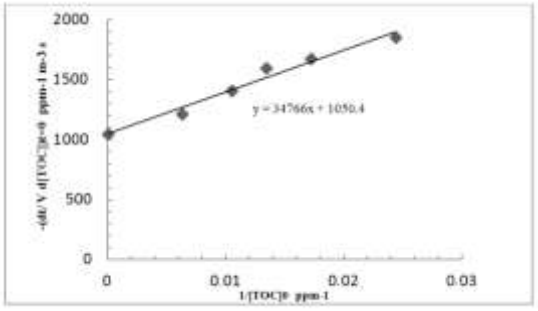

Figure 2. *Linear regression to calculate Albendazole L-H kinetic parameters*

Theoretical and experimental degradation percentages are showed in Table 3. The maximum theoretical degradation percentage was 40%, with the lowest concentration of the contaminant. Solar photocatalysis performs correctly at low pollutant concentrations as demonstrated by experimental degradation percentages. An increase of initial concentration of albendazole, causes a decrease of degradation rate. Probably, what happens is that at high concentrations, pollutant molecules cover the catalyst surface and they block the electron-hole pair formation, which is important when starting the substance degradation.

Table 3. Theoretical and experimental degradation percentage

	TOC_0 (ppm)		
	40	**75**	**159**
% degradation (Exp)	39.36	34.77	22.16
% degradation (Model)	40.52	40.52	30.52

Figure 3 shows a satisfactory settlement obtained from theoretical model and experimental data. The solid line on this figure represents values obtained from the model, while, the data points were obtained experimentally.

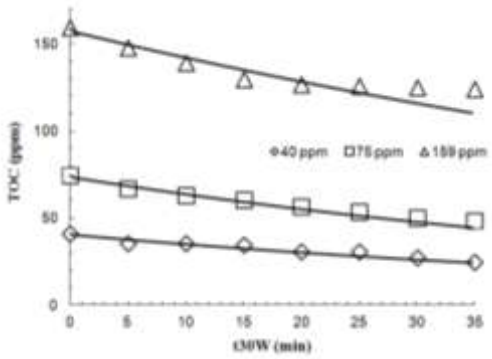

Figure 3. *Albendazole degradation curve (Theoretical vs. Experimental)*

Kinetic parameters obtained theoretically from the experimental results, are independent of the radiation field within the reactor, and they can be used in the future for scaling up applications or photocatalytic reactor design, for the same conditions and energy radiation spectrum used in this study, and for the initial pollutant concentrations and radiation intensity accumulated, that is, 35 Wh/m^2.

3.4. Optimal catalyst loading

It was found that in using 0.2 g/l catalyst loading, the highest degradation percentage were obtained for concentrations pollutants ranges used in this study. Other research concluded that the catalyst loading to optimize the degradation percentage, optimizes the absorption of photons too, which corresponds to 0.15 - 0.2 g/L interval [(28)]. Figure 4 shows the results obtained about catalyst concentration.

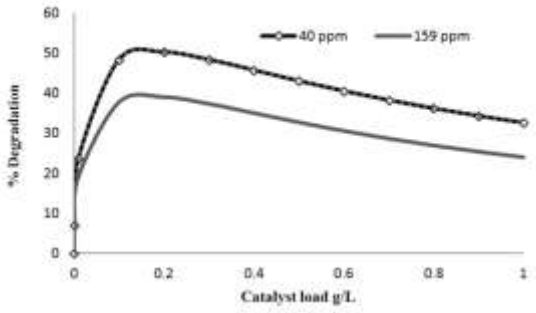

Figure 4. *Optimization of the degradation rate with catalyst loading*

An increase of the amount of titanium dioxide, favored the electron-hole pair formation. However, experimental data showed that a high catalyst loading promotes overlap, and only the upper layers receive photons directly, while the lower ones are not. As a result there is an amount of titanium dioxide that contributes to the electron-hole formation and this is directly linked with the loading value that optimizes the degradation percentage.

4. Conclusions

SFM and ray tracing articulation were accounted satisfactorily for albendazole photocatalytic degradation, as in the *LVRPA* was described appropriately along the reactor with a low catalyst loading and low contaminant initial concentration, radiant field complex geometry CPC.

Model described adequately Hilshenwood-Langmuir law degradation kinetics of albendazole. Adsorption constant (K_I) was greater than the rate constant (k_T), ensuring that limitations are not for adsorption kinetics, degradation is limitated by the reaction in the catalyst surface.

Kinetic parameters derived from fitting the model to the experimental results were independent of the radiation field in the reactor and therefore, it is found to be a suitable model for scaling photocatalytic reactors.

5. Acknowledgments

Financial support from Colciencias (Grant) is gratefully acknowledged. Colina-Márquez thank Colciencias for the financial support during their Ph.D studies and the grant No.110647922029.

6. References

(1) Alfano OM, Cassano, AE. Photoreactor Modeling: Applications to Advanced Oxidation Processes. Int J Chem React

Eng [Internet]. 2008;6(1). Available from: https://www.degruyter.com/view/j/ijcre.2008.6.1/ijcre.2008.6.1.1617/ijcre.2008.6.1.1617.xml.

(2) Spasiano D, Marotta R, Malato S, Fernandez-Ibañez P, Somma I Di. Solar photocatalysis: Materials, reactors, some commercial, and pre-industrialized applications. A comprehensive approach. Appl Catal B Environ [Internet]. 2015;170–171:90–123. Doi: 10.1016/j.apcatb.2014.12.050. Available from: https://www.sciencedirect.com/science/article/pii/S0926337315000028.

(3) Méndez-Arriaga F, Maldonado MI, Gimenez J, Esplugas S, Malato S. Abatement of ibuprofen by solar photocatalysis process: Enhancement and scale up. Catal Today [Internet]. 2009;144(1–2):112–6. Doi: 10.1016/j.cattod.2009.01.028. Available from: https://www.sciencedirect.com/science/article/pii/S0920586109000492.

(4) Radjenović J, Sirtori C, Petrović M, Barceló D, Malato S. Solar photocatalytic degradation of persistent pharmaceuticals at pilot-scale: Kinetics and characterization of major intermediate products. Appl Catal B Environ [Internet]. 2009;89(1–2):255–64. Doi: 10.1016/j.apcatb.2009.02.013. Available from: https://www.sciencedirect.com/science/article/pii/S0926337309000666#!.

(5) Puma GL, Puddu V, Tsang HK, Gora A, Toepfer B. Photocatalytic oxidation of multicomponent mixtures of estrogens (estrone (E1), 17β-estradiol (E2), 17α-ethynylestradiol (EE2) and estriol (E3)) under UVA and UVC radiation: Photon absorption, quantum yields and rate constants independent of photon absorp. Appl Catal B Environ [Internet]. 2010;99(3–4):388–97. Doi: 10.1016/j.apcatb.2010.05.015. Available from: https://www.sciencedirect.com/science/article/pii/S0926337310002146.

(6) Kasprzyk-Hordern B, Dinsdale RM, Guwy AJ. The removal of pharmaceuticals, personal care products, endocrine disruptors and illicit drugs during wastewater treatment and its impact on the quality of receiving waters. Water Res [Internet]. 2009;43(2):363–80. Doi: 10.1016/j.watres.2008.10.047. Available from: https://www.sciencedirect.com/science/article/pii/S0043135408005010.

(7) Bistoletti M, Moreno L, Alvarez L, Lanusse C. Multiresidue HPLC method to measure benzimidazole anthelmintics in plasma and egg from laying hens. Evaluation of albendazole metabolites residue profiles. Food Chem [Internet]. 2011;126(2):793–800. Doi: 10.1016/j.foodchem.2010.11.084. Available from: https://www.sciencedirect.com/science/article/pii/S0308814610015025.

(8) Pourgholami MH, Khachigian LM, Fahmy RG, Badar S, Wang L, Chu SWL, et al. Albendazole inhibits endothelial cell migration, tube formation, vasopermeability, VEGF receptor-2 expression and suppresses retinal neovascularization in ROP model of angiogenesis. Biochem Biophys Res Commun [Internet]. 2010;397(4):729–34. Available from: http://dx.doi.org/10.1016/j.bbrc.2010.06.019.

(9) Heberer T. Tracking persistent pharmaceutical residues from municipal sewage to drinking water. J Hydrol [Internet]. 2002;266(3–4):175–89. Doi: 10.1016/S0022-1694(02)00165-8. Available from: https://www.sciencedirect.com/science/article/pii/S0022169402001658.

(10) Méndez-Arriaga F, Esplugas S, Giménez J. Degradation of the emerging contaminant ibuprofen in water by photo-Fenton. Water Res [Internet]. 2010;44(2):589–95. Doi: 10.1016/j.watres.2009.07.009. Available from: https://www.sciencedirect.com/science/article/pii/S0043135409004667.

(11) Papamija M, Sarria V. Degradación fotocatalítica del ibuprofeno empleando dióxido de titanio. Rev Ing [Internet]. 2010;(31):47–53. Doi: 10.16924/riua.v0i31.211. Available from: https://ojsrevistaing.uniandes.edu.co/ojs/index.php/revista/article/view/211.

(12) Cassano AE, Alfano OM. Reaction engineering of suspended solid heterogeneous photocatalytic reactors. Catal Today [Internet]. 2000;58(2–3):167–97. Available from: https://www.sciencedirect.com/science/article/pii/S0920586100002510.

(13) Alfano OM, Bahnemann D, Cassano AE, Dillert R, Goslich R. Photocatalysis in water environments using artificial and solar light. Catal Today [Internet]. 2000;58(2–3):199–230. Available from: https://www.sciencedirect.com/science/article/pii/S0920586100002522.

(14) Toepfer B, Gora A, Puma GL. Photocatalytic oxidation of multicomponent solutions of herbicides: Reaction kinetics analysis with explicit photon absorption effects. Appl Catal B Environ [Internet]. 2006;68(3–4):171–80. Available from: https://www.sciencedirect.com/science/article/pii/S0926337306003171.

(15) Colina-Márquez J, Machuca-Martínez F, Puma GL. Photocatalytic mineralization of commercial herbicides in a pilot-scale solar CPC reactor: Photoreactor modeling and reaction kinetics constants independent of radiation field. Environ Sci Technol [Internet]. 2009;43(23):8953–60. Available from: https://pubs.acs.org/doi/abs/10.1021/es902004b.

(16) Angel-Mueses M, Machuca-Martinez F, Puma GL. Effective quantum yield and reaction rate model for evaluation of photocatalytic degradation of water contaminants in heterogeneous pilot-scale solar photoreactors. Chem Eng J [Internet]. 2013;215–216:937–47. Available from: https://www.sciencedirect.com/science/article/pii/S1385894712015616.

(17) Castilla-Caballero D, Machuca-Martínez F, Bustillo-Lecompte C, Colina-Márquez J. Photocatalytic Degradation of Commercial Acetaminophen: Evaluation, Modeling, and Scaling-Up of Photoreactors. Catalyst [Internet]. 2018;8(5):179. Doi: 10.3390/catal8050179. Available from: https://www.mdpi.com/2073-4344/8/5/179.

(18) Colina-Márquez J, López-Vásquez AF, Machuca-Martínez F. Modeling of direct solar radiation in a compound parabolic collector (CPC) with the Ray Tracing tecnique. DYNA [Internet]. 2010;77(163):132–40. Available from:

https://revistas.unal.edu.co/index.php/dyna/article/view/25545/26026.

(19) Malato S. Photocatalytic reactors for the treatment of liquid wastewater in the presence of solar irradiation. In: 1st seminar of "Advanced Oxidation Methods of the Treatment of Liquid and Air Waste" [Internet]. Greece: Aristotle University of Thessaloniki; 2004. Available from: https://www.psa.es/en/projects/cadox/documents/Solarphotoreactors.pdf.

(20) Colina-Márquez J, López-Vásquez AF, Díaz D, Rendón A, Machuca-Martínez F. Photocatalytic Treatment of A Dye Polluted Industrial Effluent With A Solar Pilot-Scale CPC Reactor. J Adv Oxid Technol [Internet]. 2016;12(1):93–99. Available from: https://www.degruyter.com/view/j/jaots.2009.12.issue-1/jaots-2009-0111/jaots-2009-0111.xml.

(21) Puma GL, Brucato A. Dimensionless analysis of slurry photocatalytic reactors using two-flux and six-flux radiation absorption–scattering models. Catal Today [Internet]. 2007;122(1–2):78–90. Doi: 10.1016/j.cattod.2007.01.027. Available from: https://www.sciencedirect.com/science/article/pii/S092058610700051X#!.

(22) Chu C, Churchill S. Multiple scattering by randomly distributed obstacles-Methods of solution. IRE Trans Antennas Propag [Internet]. 1956;4(2):142–8. Doi: 10.1109/TAP.1956.1144373. Available from: https://ieeexplore.ieee.org/document/1144373.

(23) Blanco JG, Malato S, A EC, Bandala ER, Gelover S, Leal T. Purificación de aguas por fotocatálisis heterogénea: Estado del arte. In: Blesa M, editor. CYTED - Eliminación de contaminantes por fotocatálisis heterogénea. Buenos Aires: Universidad Nacional de General San Martín; 2001. p. 51–75.

(24) Colina-Márquez J, Machuca-Martínez F, López-Vásquez AF. Fotodegradación catalítica del pesticida 2,4-d Amina 4. In Seminario Internacional: Gestión integrada de servicios relacionados con el agua en asentamientos nucleados. Santiago de Cali: Universidad del Valle; 2005.

(25) Machuca-Martínez F, Angel-Mueses M, Colina-Márquez J, Puma GL. Photocatalytic Reactor Modeling. In: Schneider J, Bahnemann D, Ye J, Puma GL, Dionysiou DD, editors. Photocatalysis: Fundamentals and Perspectives - Energy and Environment Series [Internet]. Royal Society of Chemistry; 2016. p. 388–424. Doi: 10.1039/9781782622338-00388. Available from: https://pubs.rsc.org/en/content/chapter/bk9781782620419-00388/978-1-78262-041-9.

(26) Angel-Mueses M, Machuca-Martínez F, Hernández-Ramirez A, Puma GL. Effective radiation field model to scattering – Absorption applied in heterogeneous photocatalytic reactors. Chem Eng J [Internet]. 2015;279:442–51. Doi: 10.1016/j.cej.2015.05.056. Available from: https://www.sciencedirect.com/science/article/pii/S1385894715007202.

(27) Ochoa-Gutiérrez KS, Tabares-Aguilar E, Angel-Mueses M, Machuca-Martínez F, Puma GL. A Novel Prototype Offset Multi Tubular Photoreactor (OMTP) for solar photocatalytic degradation of water

contaminants. Chem Eng J [Internet]. 2018;341:628–38. Doi: 10.1016/j.cej.2018.02.068. Available from: https://www.sciencedirect.com/science/article/pii/S1385894718302705.

(28) Colina-Márquez J, Machuca-Martínez F, Puma GL. Radiation Absorption and Optimization of Solar Photocatalytic Reactors for Environmental Applications. Environ Sci Technol [Internet]. 2010;44(13):5112–20. Doi: 10.1021/es100130h. Available from: https://pubs.acs.org/doi/abs/10.1021/es100130h.

7. Nomenclature

a SFM parameter, dimensionless

b SFM parameter, dimensionless
f friction factor, dimensionless
kT kinetic constant, mol L-1 s-1 W-0.5 m1.5
K1 binding constant, L mol-1
L reactor length, m
LVRPA local volumetric rate of photon absorption,Wm-3
m reaction order with respect to the LVRPA, dimensionless
n parameter of velocity profile for turbulent regime, dimensionless
Re Reynolds number
r radial coordinate, m
rp auxiliary coordinate in the photon flux direction,m
R reactor radius, m
t30W standardized 30 W time, s
TOC TOC concentration, mol L-1
v velocity, m s-1

7.1 Greek letters

γ SFM parameter, dimensionless
κ specific mass absorption coefficient, m2 kg-1
λ radiation wavelength, nm
θ polar coordinate, radians
σ specific mass scattering coefficient, m2 kg-1
ω scattering albedo, dimensionless

7.2 Subscripts

corr corrected
max maximum
r radial coordinate
reflected reflected radiation
R reactor
total total radiation
T Total
z axial coordinate
0 relative to incident radiation, or initial condition
λ radiation wavelength
θ angular coordinate
corr corrected

7.3 Superscripts

max maxim